

RESEARCH

Open Access



# Combination of terrestrial laser scanning and UAV photogrammetry for 3D modelling and degradation assessment of heritage building based on a lighting analysis: case study—St. Adalbert Church in Gdansk, Poland

Pawel Tysiac<sup>1\*</sup>, Anna Sieńska<sup>1</sup>, Marta Tarnowska<sup>1</sup>, Piotr Kedzierski<sup>2</sup> and Marcin Jagoda<sup>2</sup>

## Abstract

The construction of the St. Adalbert Church in Gdansk dates to 1310. It is a church of rich history and great historical value, and its care is challenging. In this study, the combination of unmanned aerial vehicle (UAV) photogrammetry and terrestrial laser scanning (TLS) was used to accurately build a 3D model of the church. Together with the collected historical inventory documentation, the historic building information model (HBIM) was generated. The Autodesk-Revit<sup>®</sup> tool was used for this purpose. On the basis of the generated model, the reflection properties of the laser scanner beam and red–green–blue (RGB) images, a methodology was proposed for analysing the degradation of the church's components. The main hypothesis of this study is based on the analysis of sunlight outside the church. In addition to the importance of the method for determining the risks of church degradation, a high-quality method for model visualization combining two photogrammetric techniques (TLS + UAV) is presented.

**Keywords** Cultural heritage, UAV photogrammetry, Laser scanning, Lighting analysis, 3D-model, HBIM

## Introduction

The development of three-dimensional models of temples, often centuries-old buildings, requires advanced technology that allows digital recording of building geometry [1, 2]. This documentation is important because objects are often exposed to deterioration due to human negligence, climate change, or natural disasters [3–5]. After obtaining detailed information on historical

buildings, it is possible to pass this information on to future generations [2]. One of the methods of obtaining spatial models is the use of remote sensing technology [6]. This technology allows us to build models based on spatial information from cameras or laser scanners [7–9]. TLS systems have been on the market for approximately 20 years and have been the standard method for acquiring 3D data for 15 years [10].

The technology of 3D modelling allows us to visualize objects and create accurate 3D models [11–13]. Modelling churches requires particular attention. It is important to create a complex and accurate model to ensure the most detailed representation of the architecture [14, 15]. Each object requires a personalized approach, and the minimum level of detail must be specified [16, 17]. Notably, 3D modelling improves the information management process during research and restoration [18].

\*Correspondence:

Pawel Tysiac  
pawtysia@pg.edu.pl

<sup>1</sup> EKO-TECH Centre, Faculty of Civil and Environmental Engineering, Gdansk University of Technology, Gabriela Narutowicza 11/12, 80-233 Gdansk, Poland

<sup>2</sup> Faculty of Civil Engineering Environmental and Geodetic Sciences, Koszalin University of Technology, Sniadeckich 2, 75-453 Koszalin, Poland



© The Author(s) 2023. **Open Access** This article is licensed under a Creative Commons Attribution 4.0 International License, which permits use, sharing, adaptation, distribution and reproduction in any medium or format, as long as you give appropriate credit to the original author(s) and the source, provide a link to the Creative Commons licence, and indicate if changes were made. The images or other third party material in this article are included in the article's Creative Commons licence, unless indicated otherwise in a credit line to the material. If material is not included in the article's Creative Commons licence and your intended use is not permitted by statutory regulation or exceeds the permitted use, you will need to obtain permission directly from the copyright holder. To view a copy of this licence, visit <http://creativecommons.org/licenses/by/4.0/>. The Creative Commons Public Domain Dedication waiver (<http://creativecommons.org/publicdomain/zero/1.0/>) applies to the data made available in this article, unless otherwise stated in a credit line to the data.

Commercial 3D modelling software allows us to build very accurate and complex models. The main problem with any software is the mapping of a geometrically incomplete object [19]. In the field of cultural heritage, 3D models are an interesting tool for built-in documentation and interactive visualization, for example, to create virtual reality environments [20–23]. 3D models obtained by laser scanning have been used to fill a virtual environment with faithful copies of real objects, such as the interior of a museum or a historic building [24–26]. Photogrammetry has been used in the 3D reconstruction of objects based on one or more images for many years [27–29]. Active sensors can generate the dense 3D point cloud data required to create high-resolution geometric models, while digital photogrammetry is more suitable for creating highly accurate textured 3D models [30–32]. BIM modelling is a digital record of the features and properties of a building object. This technology is used to visualize the object, and the created model has the actual building parameters. The essence of BIM is based on object-oriented modelling [29, 32]. Modelling cultural heritage in a BIM environment requires special attention. It is important to create an extremely complex and accurate model to ensure the most comprehensive representation of the architecture possible. Each object requires a personalized approach.

Spatial models can be used to analyse the lighting of churches. From a practical point of view, to solve the problem of detecting possible degradation, light is considered to be a direct factor. This means that if there is a shadow, the progress of degradation increases in the presence of lichens or humidity. In most cases, the method of analysing point clouds is used in the literature, but the total number of points is difficult to analyse due to their volume. This means that the analysis of lighting allows us to indicate analysis areas as the degradation progresses without having to run the entire model. The differences between the illuminated and shaded sides of an object are studied in this paper.

As shown, the general use of noninvasive methods to assess structural conditions and 3D modelling has become common in research literature [26, 33, 34]. However, the objects of study are typically engineering elements. The latest techniques present methods for determining the degree of wall degradation [35], classifying the main elements of cultural objects [36] combining photogrammetry and laser scanning measurement methods [37], and generating high-resolution 3D models using UAV techniques [38]. Our research complements each of the methods listed above. By analysing the rays of natural light falling on the church, we have developed a simple way of analysing possible places of degradation, with the additional input of a high-resolution 3D model.

To complete the analysis, we have presented measurement methods for generating high-resolution models from images and laser scanning technology. Next, we carefully performed 3D modelling in Revit software to reduce the weight of data, without information loss. The model forms the basis for planning conservation works or general facility management. We used the collected geometric and spectral information to assess the technical condition of the building and added it as an element of metadata to the model.

Based on the studies mentioned above, this paper proves that 3D modelling is important from the management perspective. Therefore, the study presents a new proposal for an inventory of temples. Our main goal is that the research results can be used by conservators or facilities managers responsible for managing churches, bearing in mind that, without a powerful workstation, they might have problems with point model analyses. The church's HBIM and the surrounding landscape are presented by combining UAV optical measurement and laser scanning technology.

## Materials and methods

### Study site and historic information

According to the legend proclaimed on the Hill of Saint Adalbert, in 997 A.D., a Czech bishop and missionary, Saint Adalbert, was killed and was first buried in Gdansk. In the twelfth century, the Benedictines came to the Saint Adalbert district, where they built a church, a monastery, and a brewery. The monks began to build a new temple in a swamp at the foot of the bishop's burial site. In 1310, excavations began, and the temple lines were defined. At the end of the fifteenth century, the Benedictines left Saint Adalbert, and the parish was taken over by diocesan priests. In 1537, the church and surrounding buildings were destroyed in a fire. The reconstruction of the temple began at the end of the sixteenth century with the help of the bishop Stanislaw Komkowski. The construction of the presbytery was completed in 1667, and in 1680, the church tower was erected. In the eighteenth century, the temple was expanded to two side chapels and received the appropriate equipment. In 1945, the sanctuary was damaged due to warfare, and it was not opened to the faithful until 1956. Currently, the temple serves as the Sanctuary of Saint Adalbert.

The building consists of a nave and two side chapels facing north and south. On the west side of the temple, a tower was added, which was a new wooden structure built without nails in 2003. The chancel is in the eastern part of the church. The sacristy is located between the chancel and the northern chapel. Between the north chapel and the nave, there is a chapel of the relics of St. Wojciech built in 1930. The church was made of



red brick and then plastered. The tower was made on a square plan. It consists of two zones: lower and upper. The lower zone—the ground floor—is very massive, while the upper floor is much narrower than the lower floor and is covered by a thick roof. The façade of the nave, presbytery, and tower is equipped with pointed windows. However, there are round arched windows in the chapel and in the upper part of the tower. Figure 1 shows the location of the church.

**Research methodology**

The research method presented in this study is based on multitechnology measurements of a temple (St. Adalbert Church in Gdansk, Poland). An UAV and a TLS were used for data acquisition. This approach gave us the opportunity to fully evaluate the measurement results. Moreover, using orthoimages allowed us to expand sunlight analyses to the immediate vicinity of the church. Figure 2 shows the workflow of this research. The workflow consists of the following:



**Fig. 1** Location of the church

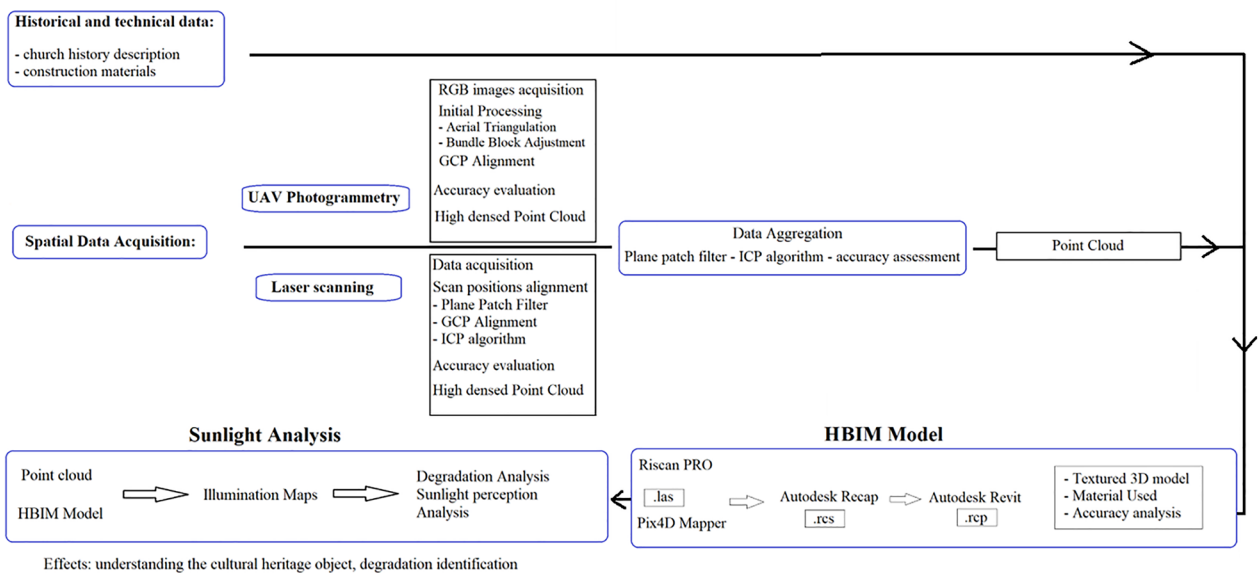


**Fig. 2** The research workflow

- (1) Acquiring all details of the historical information of the church.
- (2) Acquiring spectral and geometric information from a laser scanner and UAV photogrammetry.
- (3) Building an individual HBIM of the church based on the obtained data.
- (4) Proposing a sunlight analysis in terms of possible degradation and light perception by humans.

### UAV Photogrammetry

UAV photogrammetry was performed using a DJI Matrice 300 RTK drone and a DJI Zenmuse P1 camera. The camera has a CMOS sensor with a size of  $35.9 \times 24$  mm. The images are in .jpg format with dimensions of  $8192 \times 5460$  pixels. The focal length is 35 mm. The UAV equipment with a Global Navigation Satellite System (GNSS) and an Inertial Measurement Unit (INU) allows for direct georeferencing, which consists of measuring the position of the camera during flight. However, such positioning does not always allow for high-quality 3D reconstruction. To increase the accuracy, 18 ground control points (GCPs) were used. They were measured with a GNSS receiver—Leica CS20. The coordinate system of the images is WGS 84 (EPSG:4326). The coordinate system of the GCPs is ETRS89/Poland CS2000 zone 6 (EPSG:2177) with the EGM2008 Geoid Model. The Matrice 300 RTK is a DJI commercial drone and is part of a modern aircraft system. The company's manufacturer offers up to 55 min of flight time, advanced artificial intelligence (AI) capabilities, 6-way sensing and positioning. Brand new technology from DJI OcuSync Enterprise enables transmission distances of up to 15 kms and supports 3-channel 1080p video. Automatic real-time switching between 2.4 and 5.8 GHz allows us to fly in high-interference environments, and AES-256 encryption ensures secure data storage and transmission.

The requirements for accurate rendering and processing of high-quality 3D models are steadily increasing. For example, accurate 3D models can be used to identify potential problems in the early stages of project implementation or to complete a broader analysis of information on buildings. Therefore, vertical aerial photogrammetry cannot meet the quality requirements of the 3D model reconstruction obtained. In this research, we used oblique photogrammetry to obtain the highest data quality. Although vertical images can help show the positions of objects such as buildings relative to each other, oblique photogrammetry gives a better perspective on the appearance of objects rising above the ground. The DJI software provides the ability to use oblique images and allows us to take complete reconstruction photographs without having to carry out multiple flights, as shown in [39].

The images were processed in PIX4DMapper software. The church was photographed with 36 images. During processing, 3 stages were used: initial processing, point cloud and mesh creation and orthomosaic and digital surface model (DSM) creation. Initial processing was based on acquiring information about image alignment results (so-called automatic tie-points) and then determining the elements of internal and external orientation and aligning them to manually measured control points (GCPs). After the processing steps, the acquired point cloud was saved in .las format. To correctly show the accuracy of the results, the position error between the control points (those that did not participate in the alignment and those that were obtained from the images) is shown in Table 1. Considering that the study area was about  $5,000 \text{ m}^2$  and had dimensions of about  $60 \text{ m} \times 85 \text{ m}$ , and the flight altitude was 100 m, we were able to perform the study using vertical and oblique images. The GSD was about 1 cm. The results of bundle block adjustment and resulting point cloud showing the church and its surroundings is given in Fig. 3.

**Table 1** Localisation accuracy per GCP and mean errors in the three coordinate directions

| Check Point Name | Error X [m] | Error Y [m] | Error Z [m] | Projection Error [pixel] | Verified/<br>Marked<br>Images |
|------------------|-------------|-------------|-------------|--------------------------|-------------------------------|
| 1                | 0.0203      | 0.0008      | - 0.1251    | 0.3605                   | 3                             |
| 2                | - 0.0192    | 0.0575      | 0.0375      | 0.2295                   | 4                             |
| 3                | 0.0292      | - 0.0200    | - 0.0029    | 0.4569                   | 4                             |
| 4                | 0.0021      | 0.0115      | 0.0655      | 0.3030                   | 6                             |
| 5                | 0.0228      | 0.0138      | 0.0184      | 0.2115                   | 4                             |
| Mean [m]         | 0.011032    | 0.012712    | - 0.001341  |                          |                               |
| Sigma [m]        | 0.017591    | 0.025388    | 0.065845    |                          |                               |
| RMS Error [m]    | 0.020764    | 0.028392    | 0.065859    |                          |                               |





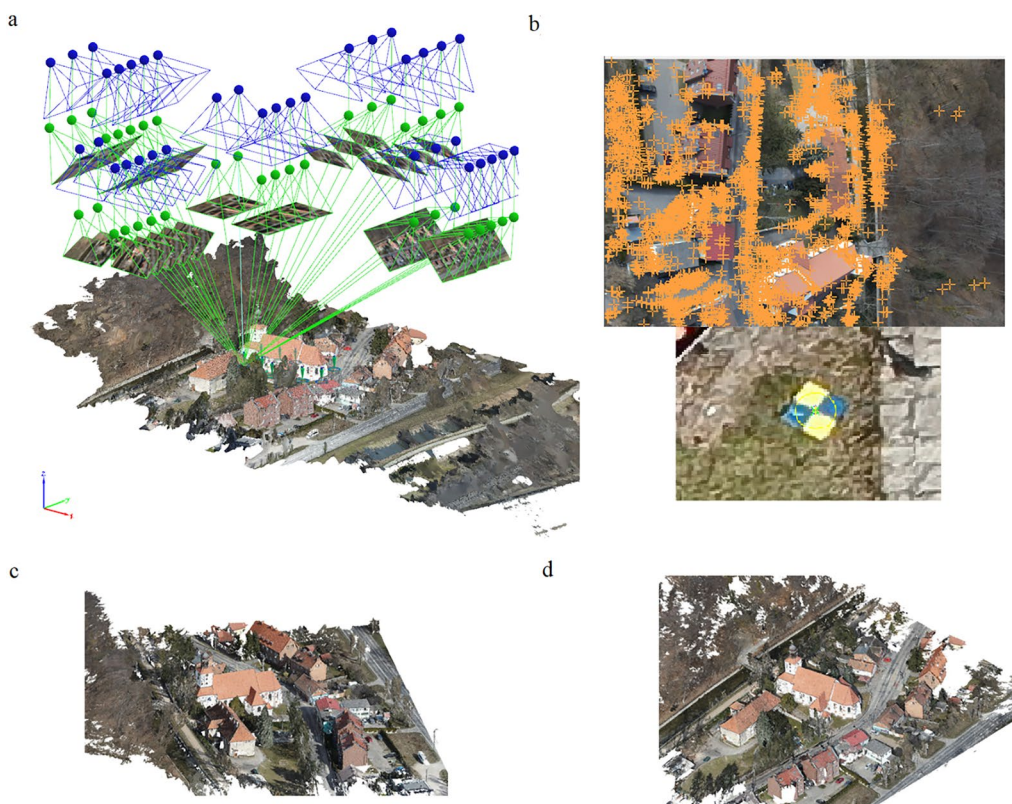


**Fig. 3** a Bundle block adjustment results, b automatic tie-points and GCP, c, d UAV oblique photogrammetry results

### Terrestrial laser scanning (TLS)

Laser scanning measurements were made with a Leica Scan Station P30. This is a Light Detection and Ranging (LIDAR) scanner with an ultrafast pulse method (the device is able to collect up to 1 million points per second). The presence of a digital camera makes it possible to assign specific RGB colours to the point cloud. This type of scanner is a very good solution for working with large objects. The accuracy of the results obtained is satisfactory (reaching 1 cm), and the measurement itself is relatively simple. This instrument is ideally suited for scanning 3D geometry and generating data for integration with a building information modelling system. As noted in the literature [34], the use of laser scanning is associated with certain limitations. For example, the point cloud may contain many unnecessary elements and noise. In our case, the main obscuring elements were trees on the northwest and west sides. Another problem with laser scanning is the occurrence of blind spots due to obstructions or undesirable measurement conditions. Therefore, it is not always possible to scan the entire object. To avoid this problem, we used UAV oblique photogrammetry.

In order to present the possibilities of using the laser scanner more broadly, we have presented the location of the scanner during the measurements in Fig. 4. According to the Fig. 4, scan positions around the church are numbered from 1 to 13. Additional scan positions from 14 to 20 were located inside the church. Denser distribution of scanner positions around the tower was



**Fig. 4** Scan positions location

because the scanner was located in close proximity to the church. This was for two reasons: first, to combine the scans recorded outside and inside the church, we needed to have as many common elements as possible to minimize an alignment error. Second, we used the beam reflection intensity for our analyses. Due to the fact that its value also depends on the angle, the type of material, its colour and humidity, we didn't want the angle of a laser beam to be perpendicular to the church (which has the effect of too high intensity value saturation) or too large (where the laser beam won't be able to return to the scanner).

The most important feature of the scanner used in this research is the possibility of precise measurements, with a precision of several millimetres, and the possibility of registering the intensity of the light-beam reflection. Our experience shows that, despite the limitations, scanning a building provides products of better quality than photogrammetry does (e.g., due to the accuracy of edge registration). This has been demonstrated in the literature by, among others, Mohammadi et al. [40] and Moon et al. [41]. Therefore, two assumptions were made during the field survey. The first determined the visibility of the scanner positions relative to each other, and the second determined the maximum distance from the measured object. In exceptional places (i.e., in scan position alignment between points outside and inside the church), the density of the positions was increased to record the tie-points (tie-points are the points that align

individual scanner positions to each other) as accurately as possible. Moreover, as in the case of UAV oblique photogrammetry, manual and automatic filtered tie-points were used to align the data to the same coordinate system (ETRS89/Poland CS2000 zone 6 (EPSG: 2177) and the EGM2008Geoid model). In this way, we obtained two photogrammetric models in relatively close proximity. The registration process was performed in RiSCAN PRO<sup>®</sup> software. This process was based on corresponding tie-points (created automatically or indicated manually). To minimize alignment errors, RiSCAN PRO<sup>®</sup> has a plugin function called "Multi-Station Adjustment" (MSA). The main functionality of MSA is to improve the registration of scan positions. For that purpose, the external position of each scan position was modified to calculate the best overall fit for them. The alignment results are shown in Fig. 5 as a histogram of the residues of the tie-points and an error sphere.

In Fig. 6, the resulting point cloud is shown in RGB colours and as the intensity of the beam reflection from the object.

#### TLS and UAV photogrammetry aggregation

After obtaining point clouds from both TLS technology and UAV photogrammetry, registration to the same coordinate system ensured a relatively close positioning of the point clouds. However, when acquiring a spatial model, one of the objectives was to create the point cloud model with the highest possible accuracy for the BIM modelling

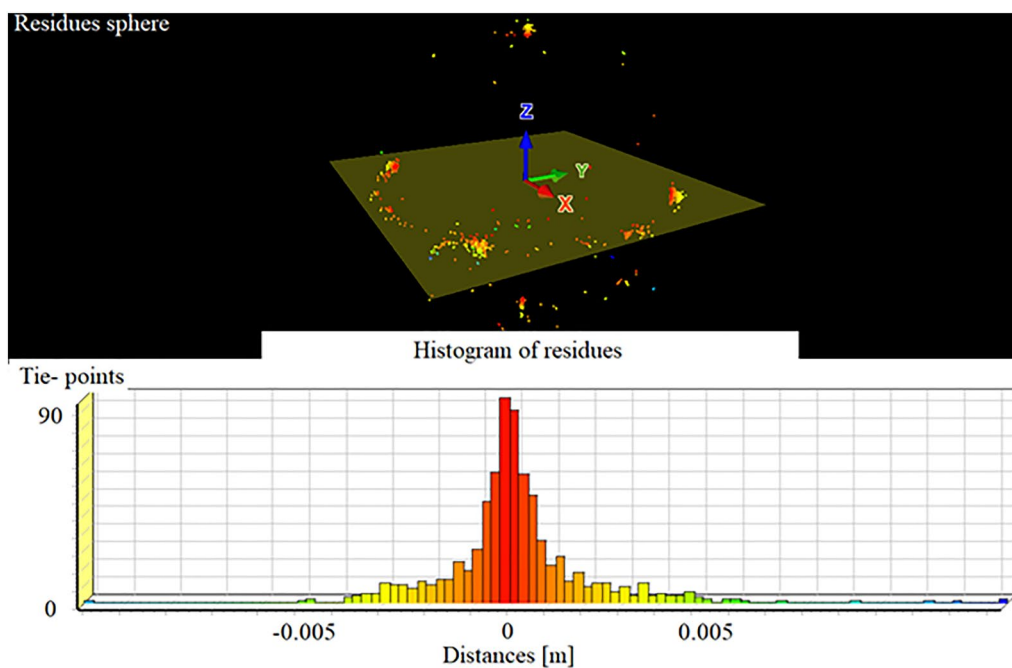


**Fig. 5** TLS Alignment results as a histogram of residues between tie-points



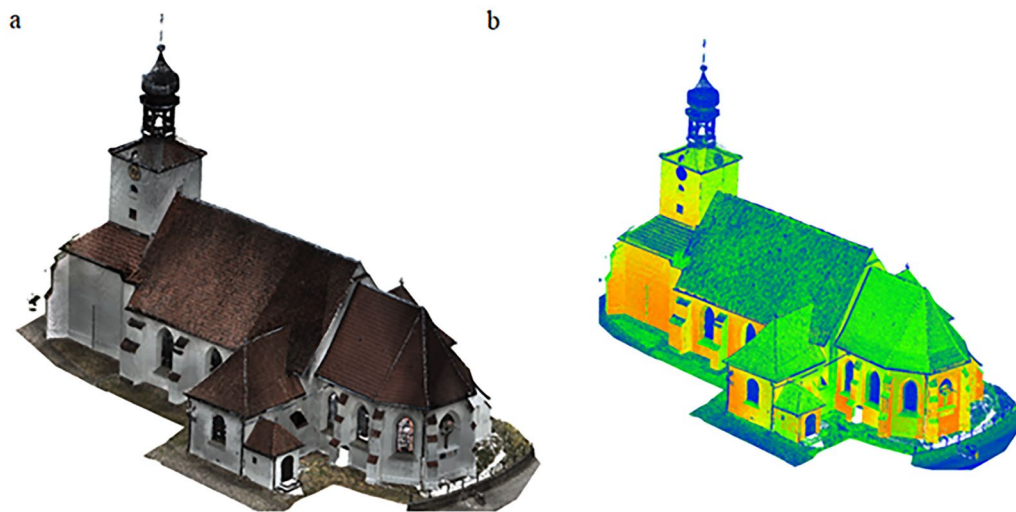


**Fig. 6** TLS point cloud in **a** RGB colours and **b** the Intensity of the beam reflection

stage. For this purpose, we used Riscan Pro<sup>®</sup> software. This software has the plane patch filter algorithm, which together with the iterative closest points (ICP) algorithm aligned the clouds of points with each other. The plane patch filter algorithm divides the point cloud into smaller cubes and then searches for the best-fitting plane inside these cubes using least-squares adjustment. When the algorithm finds the best-fitting plane, it estimates the location of the centre of gravity, which, together with the normal vector, is stored on a hard disk. The ICP algorithm then aligns these points; it is one of the most popular methods in point cloud alignment [42, 43]. The standard deviation obtained as the final result of this operation did not exceed 1 cm between the tie-points. The principle of point cloud aggregation is the same as in the case of combining scan positions from a terrestrial laser scanner, presented in this study. We present the result of this combination as an open access data [44].

#### HBIM methodology

The modelling phase was carried out with Autodesk Revit<sup>®</sup>, a type of building information modelling software. After the point cloud has been properly imported, the church modelling stage in the Revit environment must start by adding levels to which the whole BIM work process must refer. Then, the added levels are automatically used to create a floor plan associated with them. The projection is a 2D view of the model display, forming the basis for placing the church's individual parts. In historic buildings, walls are often heterogeneous in thickness, lack horizontality, and show deviation. In most cases, therefore, individual elements are modelled manually. To save time and reduce the manual modelling for all

elements, some elements use rules derived from experience. For example, if the angle of the individual roof slope relative to the horizontal plane generated from the point cloud is measured, the end point of the roof slope curve can be predicted. In a specific level projection, a closed loop of the roof boundary was designed, and its slope was defined. Its value was then changed to reproduce the structural elements as faithfully as possible, depending on the ordering of points.

The technical elements obtained from the documentation were modelled in two ways. First, a large family library was built, making modelling faster. For example, a new family is created for windows that use the same family in multiple situations. One of the challenges in the modelling stage was the entrance to the church. Separately, the white decorative elements around the entrance were made along the same path as the muntin bars. A wooden door was inserted into the opening, and the size was determined by drawing the perimeter on the point cloud. We marked elements determining material differences by analysing the range of reflection spectra of the laser scanner and RGB colour ranges. The results of this review are shown in Table 2. There, the range of the reflection intensity for individual materials is quite large, but these are the extreme values that occurred in the measurements. Moreover, we noticed that each material had an average value, which occurred most often. Due to the significant tonal differences in the cloud of points, it was possible to adapt a specific material and precisely determine where a given element occurred, e.g., for walls that clearly differed in shade from the rest of the object. After registration, the actual surface of the object could be obtained, and the state of degradation could be



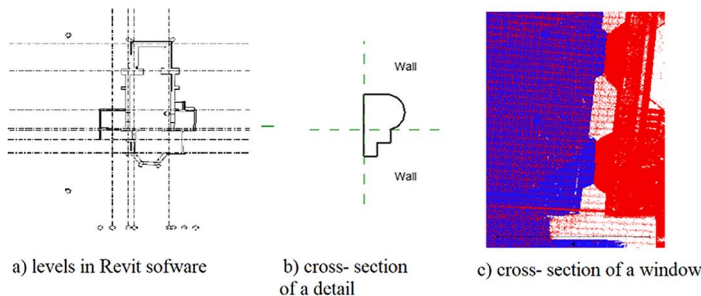
**Table 2** Material characteristics based on an intensity beam reflection and an RGB Colour Dynamic

| Material Type | Laser Scanning Intensity [0–1] |      | RGB Colour Dynamic [0–255] |        |        |
|---------------|--------------------------------|------|----------------------------|--------|--------|
|               | Range                          | Mean | R                          | G      | B      |
| Glass         | 0.03–0.09                      | 0.05 | 12–115                     | 12–116 | 12–120 |
| Plaster       | 0.33–0.90                      | 0.72 | 23–249                     | 23–249 | 23–249 |
| Wood          | 0.03–0.10                      | 0.05 | 6–27                       | 6–27   | 6–27   |
| Old Tile      | 0.07–0.50                      | 0.23 | 9–113                      | 9–113  | 9–113  |
| New Tile      | 0.07–0.38                      | 0.21 | 23–42                      | 23–42  | 23–42  |

analysed. It should be noted, however, that the intensity of the beam reflection is affected not only by the type of material, but also by its colour, structure (roughness) and humidity. Therefore, the values presented by us helped us to classify the material of the church elements, but they cannot be used as reference values for other objects. For each measurement, a separate analysis should be made of the dependence of the material on the intensity of reflection due to variable humidity, structure and colour, e.g., of wood. The modelling workflow is shown in Fig. 7.

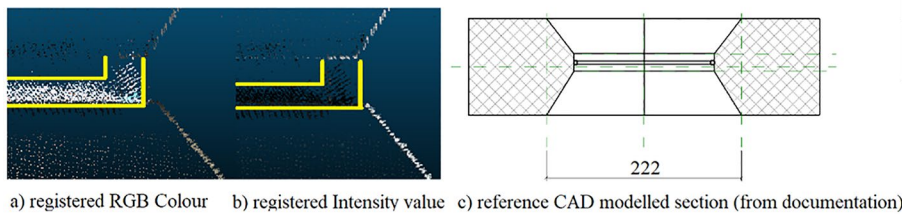
**Step 1**

Setting up levels, planes, vertical sections and cross sections



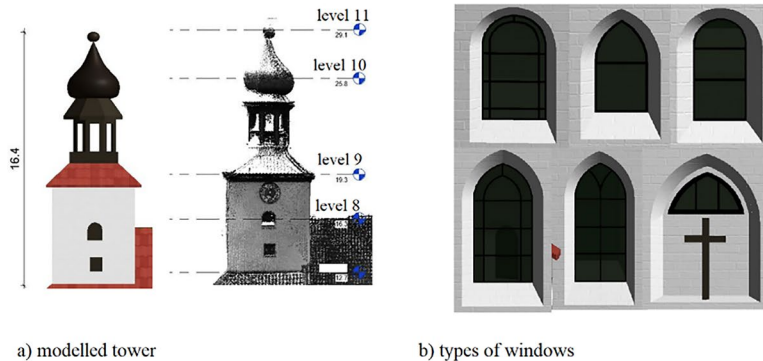
**Step 2**

Material Components Library



**Step 3**

Create Families and Individual Components



**Step 4**  
Generate 3D model

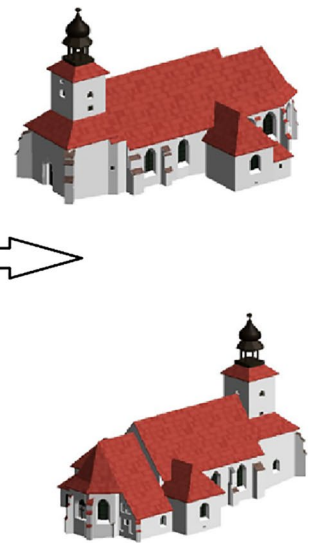


**Fig. 7** The HBIM Model generation workflow



### Sunlight analysis based on 3D models

The sun's rays that cross the sky change their position with the passing of the seasons, from winter through spring, summer and autumn. The length of the day, the height of the sun in the sky, and the intensity of the sunlight change. At the equator, these changes are slight, but they change more drastically closer to the poles. They define life on Earth, from plants and animals to humans. In our analysis, the tests were performed at the autumn equinox (September 23), the spring equinox (March 20), and on the first day of winter (December 21) and summer (June 21). The same time was adopted for all dates—12:00 p.m. By analysing the trajectory of the light at different seasons of the year, the shadows cast by the church were analysed, showing that places with darkness are more likely to be degraded. An additional finding of the conducted analyses is the theoretical increase in humidity in places of continuous shade. This can cause the appearance of lichen on the building or cause faster material fatigue. Numerous insolation analyses not only of the church but also of the immediate vicinity using ArcMap<sup>®</sup> software were performed to obtain the effects in specific places, which were later subjected to more detailed analysis. This approach allowed us to analyse possible terrain obstacles that may obstruct the light from reaching the church. In dark places, we analysed the intensity of the beam reflection. Moreover, we calculated the metric deviations from the reference model that we obtained in 2017 (results not published). The HBIM lighting analysis was performed in Revit<sup>®</sup> software, and the church and its surroundings were analysed in ArcMap<sup>®</sup> software. We used the model illumination options available in these software packages.

### Results

In the case of lighting analysis, the object was illuminated during the spring and fall equinoxes, then during the summer solstice and the winter solstice. The results are shown in Fig. 8.

As seen in Fig. 8, the northern façade remains without access to sunlight in all four cases. During the summer, when the sun rises above the horizon, it reaches much closer to the wall but does not fall directly onto it. On this day, it can be concluded that the northern façade receives the greatest amount of light dispersed in the atmosphere. The opposite of the abovementioned situation is the winter solstice. During this period, sunlight does not reach the northern lobe of the roof. Furthermore, the southern facade is poorly illuminated during this period, as the ray angle is small, and thus, the shadow generated by the surrounding objects is large. The images that show the insolation during the equinox are identical. As seen in Fig. 7,

the illumination of the church is strongly influenced not only by its orientation but also by the heights and positions of neighbouring objects such as buildings and trees. Figure 8 shows that the lighting is affected by objects to the east and south of the object under study. As representative examples, we performed a spectral and geometrical analysis of the places with the smallest coefficients in each of the periods. Thus, we emphasize comparative analysis and propose an idea for how to analyse possible degradations of cultural objects with little documentation but rich histories.

To properly analyse the model, we performed a sun trajectory analysis every 2 h from 08:00 a.m. to 6 p.m. Then, we numbered the windows according to Fig. 9. The results of sunlight reaching these windows are presented in Table 3. Before 08:00 a.m., the sun's rays reach only windows 1–3, located on the chancel, in autumn, spring and summer, while in summer, when the sun is higher, it also reaches windows No. 4–6, located in the southern part of the church. Between 08:00 a.m. and 10:00 a.m., from autumn to spring, the sun reaches windows 1–3, but windows 4–6 are also lit at the same time in summer. Between 10:00 a.m. and 2:00 p.m. throughout the year, the sun's rays reach all windows on the south side. From 2:00 to 4:00 p.m., windows 1 and 2 are illuminated year round, while in spring and autumn, natural light also reaches window no. 5, located in the presbytery. From spring to winter, after 4 p.m., the sun's rays reach the interior of the church through the entrance door on the west side of the church. In the summer, when the sun goes down later than during the rest of the year, after 6 p.m., the sun's rays reach windows 10 and 11 on the north side. To ensure the deepest possible lighting analysis, we checked the most shady areas for moisture, lichen and geometric deformation. The results are presented in Fig. 10 and Fig. 11.

As shown in Fig. 10, there are visible differences in the intensity of beam reflection between the illuminated and shaded sides. In the places marked “1” and “2” (based on the analysis shown in Fig. 8), these differences are the greatest. The intensity of the shade in these places indicates that the possible humidity and the appearance of moss may affect the quality of the material. To draw the appropriate conclusions from the method presented in the article, a geometric analysis was performed. The results were compared between the shaded and illuminated parts of the church. To obtain suitable data for the analysis, the point cloud was filtered and triangulated, and the calculation was performed by estimating the distances between the reference data from 2017 and our model. The results of this analysis are presented in Fig. 11. The differences are not significant. The largest deviations are located in places with year-round shade

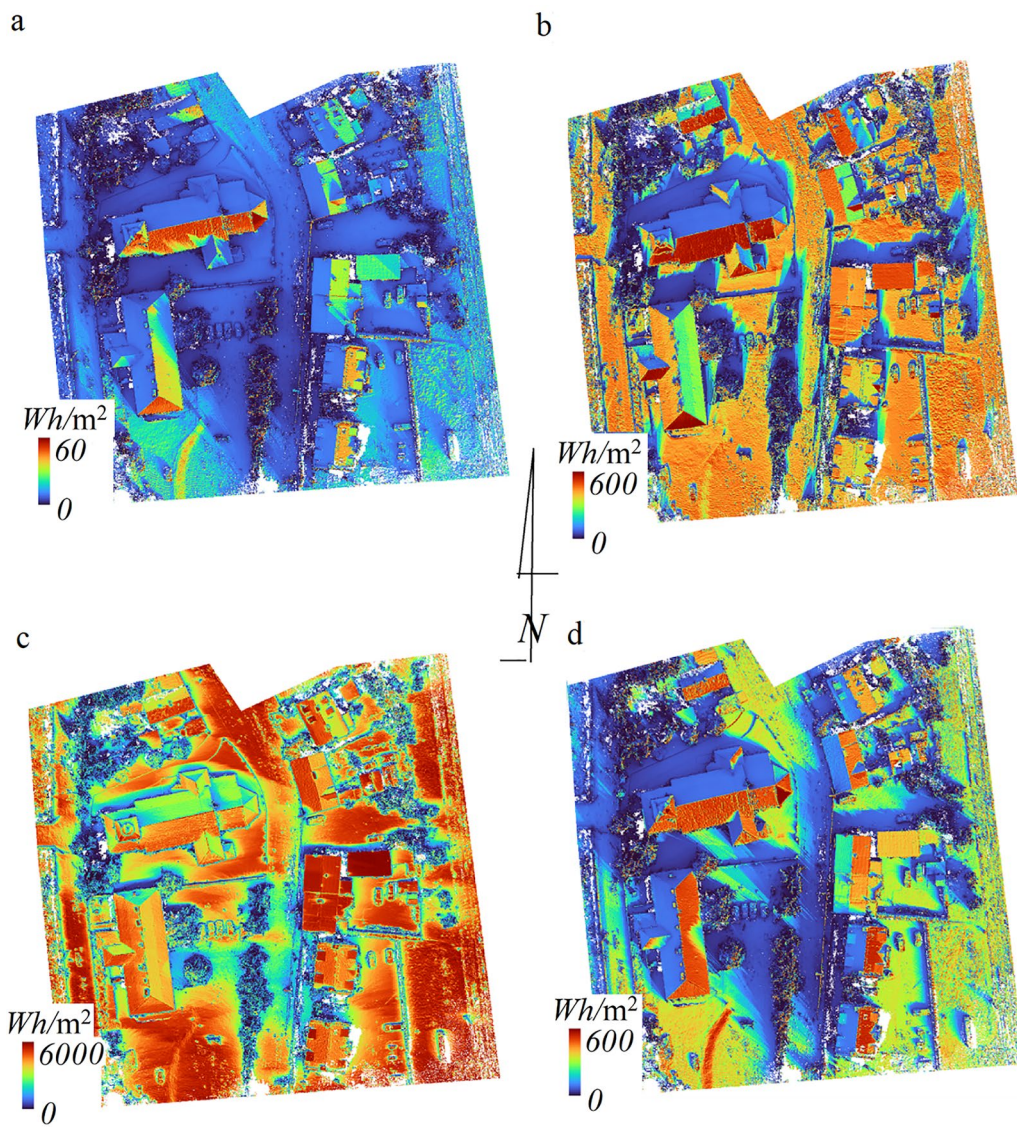


**Fig. 8** Insolation results in ArcMap® software **a** 21st December; **b** 20th March **c** 21st June **d** 23rd September

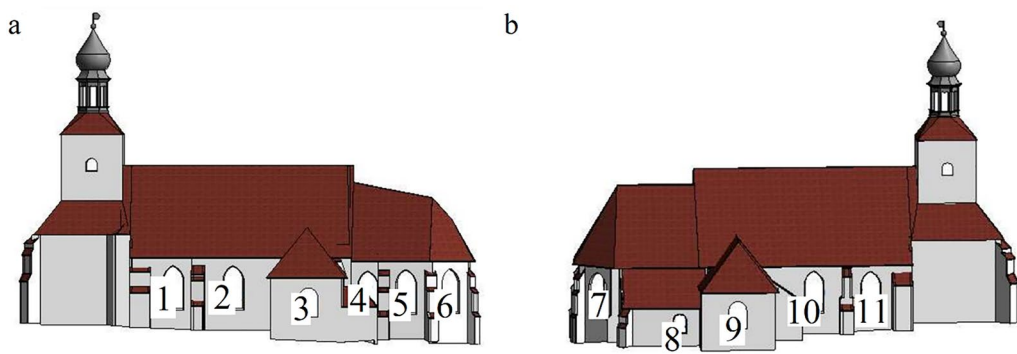
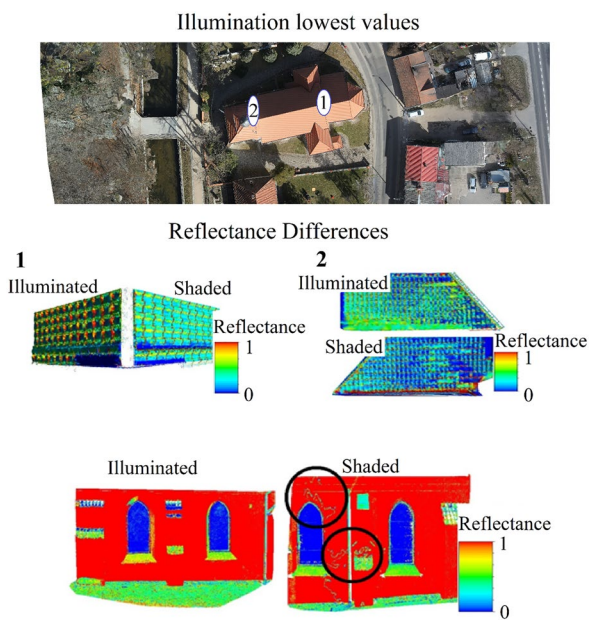


**Fig. 9** Window numeration **a** south elevation, **b** northern elevation



**Table 3** List of window openings reached by solar radiation

| Date hour            | March 20/<br>September 23 | June 21 | December 21 |
|----------------------|---------------------------|---------|-------------|
| < 8:00 a.m           | 1–3                       | 1–6     | –           |
| 8:00 a.m.–10:00 a.m  | 1–3                       | 1–6     | 1–3         |
| 10:00 a.m.–12:00 a.m | 1–6                       | 1–6     | 1–6         |
| 12:00 a.m.–2:00 p.m  | 1–6                       | 1–6     | 1–6         |
| 2:00 p.m.–4:00 p.m   | 1, 2, 5                   | 1       | 1, 2        |
| 4:00 p.m.–6:00 p.m   | –                         | –       | –           |
| > 6:00 p.m           | –                         | 10, 11  | –           |

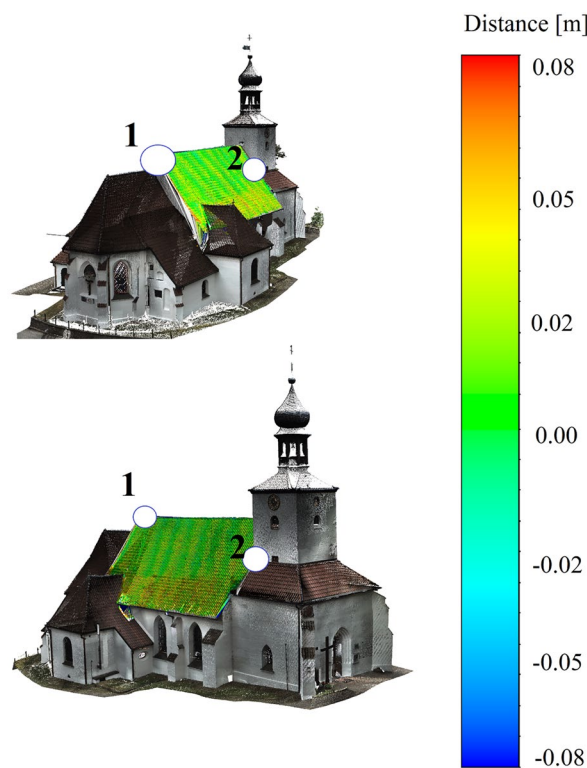


**Fig. 10** Reflection beam analysis in the locations with the smallest illumination values

and are not more than 3 cm. On the illuminated side, no differences were observed over 5 years.

**Discussion**




In this research, two measurement methods (TLS and UAV photogrammetry) were used to obtain reference data for the analysis and 3D modelling processes. First, it is worth noting that the approach of using both remote sensing techniques has been described in previous literature. For example, Valenti and Paterno [41] wanted to show which of these methods is better by showing the advantages and disadvantages of each of them. Since TLS and UAV photogrammetry are different in terms of data quality, they are best viewed as aggregated. Therefore, acquiring the reference data with their characteristics (i.e., TLS intensity or RGB values for models obtained from the images) allowed us to identify threats in terms of the durability of a



**Fig. 11** Geometric differences results on the roof's shaded side

church. In summary, this makes this method an ideal basis for the development of BIMs. When reviewing previous research on similar approaches, we found that Adami [24] and Remendino [26] raised an issue that we needed to take into account. They examined the geometric properties of the point clouds obtained in relation to the created 3D model. To address the important issue raised, we conducted an accurate analysis of each remote sensing product, and in difficult modelling areas, we did not apply generalizations but rather performed manual modelling to reproduce the model as accurately as possible. Therefore, the 3D model was the basis for further analysis and served as a major database for planning future renovation projects or determining the type of material that would be fatigued. The model created in this way is the basis for supplementing the model metadata with subsequent numerical analyses (e.g., presented in Fig. 12), and will be the basis for future research. This will focus on the universality of using the model for the largest possible group of recipients. Therefore, we tried to reduce its weight on the hard disk (for example: the mesh model of the whole church is much heavier in operations than the model created in Revit). One of the assumptions is also an attempt to introduce Community Science [45], where the model can be supplemented with elements made by



| Property                             | Image Proof   |
|--------------------------------------|---|
| Old and New Tile                     |  |
| Brick filled elements                |  |
| Plaster thickness<br>(Visible brick) |  |

**Fig. 12** Noted discontinuities from the HBIM and evidence in the form of photographic documentation

people who create a community around the church. In our opinion, the use of such a solution may reduce the obligation of cyclical measurements, if the documentation, e.g., in photographic form, will be supplemented.

Analysing the results we achieved, we noticed that our solution introduces a new quality in relation to the latest research results [35–38]. For each of the above items, we found additional values that our article introduces:

- Firstly, lighting analysis based on the analysis of the intensity of the electromagnetic wave can be the basis for classification using machine learning techniques regarding the possible degradation of a historical object.
- Secondly, the combination of UAV and LiDAR involved establishing the same system for external targets (tie-points). During the complex construction of a temple, however, it requires time and taking a large number of images. In our approach, there are only 36 images, and the reference was based on the ICP algorithm using the Plane Patch Filter method. This alignment can be described as semi-automatic, and a specific exact statistical test for the precision of the alignment provides much more confidence than the one for control points,
- Thirdly, we generated a complex 3d model of the church and, based on the obtained model, we proposed a numerical method based on a beam reflection intensity and comparisons between planes model to see if the degradation occurs.

The compliance issues described above allowed us to develop the HBIM using available materials. In the case of this particular temple, no regular monitoring is carried out, and renovation works are performed on the basis of visual inspection only after degradation has occurred. By using our idea of building a database for the analysis of lighting in the church and its immediate surroundings, we believe that a solid basis has been established to classify shaded locations based on models and to complete the necessary documentation (e.g., of the condition of the roof and tiles and the occurrence of humidity, lichen, and material fatigue). In this case, documentation, such as photographs, can be obtained by the manager of the facility, and material analysis can be carried out by a project specialist based on those photographs. This will help save time while maximizing the safety of the facility. According to the analysis performed and the addition of information on the intensity of the electromagnetic waves to the model, we noticed several elements of the church that might not be seen during a comprehensive visual inspection. We show this in Fig. 12 by naming the materials observed in the analysis and providing photographic evidence as an implementation of the method of managing a cultural building.

In our case study, an analysis of sunlight for the church and its immediate surroundings showed that there are places where sunlight never reaches during the year. We classified these places and adjusted them in our model on the basis of the results shown in Fig. 8. In this way, the following building management thesis can be put forward: if the illumination value is the smallest in the analysis, there is the greatest possibility of degradation. The spatial arrangement of the church indicates that one side of the church (northern) is not illuminated at all, and the presence of large vegetation (trees) increases the humidity there. We have shown that this is significant, since a higher humidity appears in Fig. 10 that deserves much attention for possible degradation monitoring. The church wall itself is 60 cm thick, so only the top part can be noticeably degraded, but it is often the case that the under-plaster moisture affects a much larger area than is noticeable. Renovation works in this area are associated with high costs and the need to apply for permission to carry out maintenance due to the level of building degradation. In addition, our idea has been supported in the literature by a religious analysis in the case of sunlight. Carlos [43] and Mukherji [44] presented an example of such research. They focused on how light enters a church and how it affects the intentions of the faithful.

## Conclusions

It is generally accepted that high-resolution methods for building object information databases require high computing power and high operator skills. We agree with this statement, but only at the beginning of working on a project. After creating a database and preparing the management material as an HBIM, any user can handle the work of a project of this type. It is also possible to work in the cloud, making it very convenient to manage such data. It should be noted that noninvasive measurement methods such as TLS and UAV photogrammetry are the best solutions when studying cultural heritage sites, as they allow us to acquire accurate data without interfering with the measurement object. The 3D modelling process is complicated from the perspective of building the 3D model. Its individual characteristics, however, ensure a high degree of certainty in the case of facility management. Caring for our common history is extremely important; therefore, modern technologies must be fully used, and ideas for building databases must be supported by arguments and analysis. In view of this, our work has many advantages. A 3D model was built based on the most modern measurement solutions to show the aggregation of the results (TLS + UAV). Moreover, the idea of building a database was demonstrated based on the sunlight analysis of the church and its surroundings, in addition to the implementation of materials indicated in the temple's documents.

This study provides a practical and easy to implement research idea for 3D modelling, UAV photogrammetry and TLS aggregation measurements and degradation analysis. Based on the presented research and results, it can be seen that the method presented in the article is suitable for conservation and architectural studies. From the technical side, it can be useful for any kind of renovation work or church expansion, as well as for arranging the space around the church in such a way that the light inside remains unchanged or improves. During the study, it was observed that the roof structure on the shaded side may degrade more quickly. However, drawing such conclusions requires further study of the temple. Therefore, as an additional element, the article mentions the greatest possible reduction of research in order to try to introduce Community Science, which will be an additional element of analysis and research on the presented church.

## Abbreviations

|       |                                     |
|-------|-------------------------------------|
| UAV   | Unmanned aerial vehicle             |
| TLS   | Terrestrial laser scanning          |
| BIM   | Building information model          |
| HBIM  | Historic building information model |
| ICP   | Iterative closest points            |
| RGB   | Red–Green–Blue                      |
| LiDAR | Light detection and ranging         |

|      |                                       |
|------|---------------------------------------|
| EPSG | Geodetic parameter dataset            |
| GNSS | Global navigation satellite system    |
| IMU  | Inertial measurement unit             |
| 3D   | Three dimensional                     |
| 2D   | Two dimensional                       |
| GCP  | Ground control point                  |
| ETRS | European Terrestrial Reference System |
| EGM  | Earth gravitational model             |
| MSA  | Multi-station adjustment              |

## Acknowledgements

The support of these studies by Gdansk University of Technology under the DEC-26/2021/IDUB/1.3.3 grant under the Argentum Triggering Research Grants—'Excellence Initiative—Research University' program is gratefully acknowledged. A note of gratitude is also due to all those who were involved in the research for their participation in the present study, particularly to PhD. Eng. Paweł Burdziakowski for his assistance.

## Author contributions

Conceptualization, PT; methodology, PT; software, PT, AS, MT, PK; validation, PT; formal analysis, PT, PK; investigation, PT; resources, PT; data curation, PT, AS, MT; writing—original draft preparation, PT, PK, MJ; writing—review and editing, PT, PK, MJ; visualization, PT, PK; supervision, PT; project administration, PT; funding acquisition, PT. All authors read and approved the final manuscript.

## Funding

Not applicable.

## Availability of data and materials

The datasets used during the current study are available from the corresponding reference: Tysiac P. St. Adalbert church 3D point model [dataset]. Gdansk University of Technology. 2023; <https://doi.org/10.34808/6hsv-Ds40>.

## Declarations

### Competing interests

The authors declare no competing interests.

Received: 7 November 2022 Accepted: 1 March 2023

Published online: 15 March 2023

## References

1. Kwoczynska B, Piech I, Polewany P, Gora K. Modeling of sacral objects made on the basis of aerial and terrestrial laser scanning. In: 2018 Baltic geodetic congress (BGC Geomatics). 2018. p. 275–82. <https://doi.org/10.1109/BGC-Geomatics.2018.00059>.
2. Remondino F. Heritage recording and 3D modeling with photogrammetry and 3D scanning. *Remote Sens.* 2011;3(6):1104–38. <https://doi.org/10.3390/rs3061104>.
3. Stojaković V, Tepavčević B. Optimal Methodes For 3D modeling of devastated architectural objects. In: ISPRS Archives—Vol. XXXVIII-5/W1, 2009.
4. Zaplata R. Non-invasive methods in the study and documentation of cultural heritage: aspects of laser scanning in archaeological and architectural research. Warsaw: Fundacja Hereditas; 2013.
5. Münster S, Koehler T. 3D reconstruction of cultural heritage artifacts: a literature based survey of recent projects and workflows. In: Hoppe S, Breitling S, editors. *Virtual palaces, Part II. Lost palaces and their afterlife virtual reconstruction between science and media.* Heidelberg: Paladium; 2016. p. 87–102.
6. El-Hakim SF, Beraldin JA, Picard M, Vettore A. Effective 3D modeling of heritage sites. In: *Fourth International Conference on 3-D Digital Imaging and Modeling, Banff, Canada. 06–10 Oct 2003.* p. 302–9. <https://doi.org/10.1109/IM.2003.1240263>.
7. Kedzierski M, Walczykowski P, Fryskowska A. Some aspects of architectural documentation of cultural heritage objects (In Polish: Wybrane Aspekty Opracowania Dokumentacji Architektonicznej Obiektów Zabytkowych). *Arch Photogramm Cartogr Remote Sens.* 2008;18a:221–30.



8. Bartonek D, Buday M. Problems of creation and usage of 3D model of structures and theirs possible solution. *Symmetry*. 2020;12:1. <https://doi.org/10.3390/sym12010181>.
9. Pawłowicz JA. Importance of laser scanning resolution in the process of recreating the architectural details of historical buildings. *IOP Conf Ser: Mater Sci Eng*. 2017. <https://doi.org/10.1088/1757-899x/245/5/052038>.
10. Kersten TP, Mechelke K, Lindstaedt M, Sternberg H. Methods for geometric accuracy investigations of terrestrial laser scanning systems. *Photogramm-Fernerkund-Geoinform*. 2009;4:301–15. <https://doi.org/10.1127/1432-8364/2009/0023>.
11. Smith DK, Tardif M. *Building information modeling: a strategic implementation guide for architects, engineers, constructors, and real estate asset managers*. New Jersey: Wiley; 2009.
12. Yang T, Liao L. Research on building information model (BIM) technology. *World Constr*. 2016;5:1. <https://doi.org/10.18686/wcj.v5i1.1>.
13. Morita M, Bilmes G. Applications of low-cost 3D imaging techniques for the documentation of heritage objects. *Optica Pura Aplicada*. 2018;51:1–11. <https://doi.org/10.7149/OPA.51.2.50026>.
14. Stylianidis E, Remondino F. Basics of photography for cultural heritage imaging; basics of image-based modelling techniques in cultural heritage. In: Stylianidis E, Remondino F, editors. *3D recording, documentation and management of cultural heritage*. Dunbeath: Whittles Publishing; 2016.
15. Bernardini F, Rushmeier H, Martin I, Mittleman J, Taubin G. Building a digital model of Michelangelo's Florentine Pieta. *IEEE Comput Graphics Appl*. 2001;22:59–67. <https://doi.org/10.1109/38.974519>.
16. Adami A, Scala B, Spezzoni A. Modelling and accuracy in a BIM environment for planned conservation: the apartment of Troia of Giulio Romano. *ISPRS-Int Arch Photogramm Remote Sens Spatial Inf Sci*. 2017;XLII-2/W3:17–23. <https://doi.org/10.5194/isprs-archives-XLII-2-W3-17-2017>.
17. Guidi G, Beraldin J, Atzeni C. High-accuracy 3D modeling of cultural heritage: the digitizing of Donatello's "Maddalena." *IEEE Trans Image Process*. 2004;13:370–80. <https://doi.org/10.1109/TIP.2003.822592>.
18. Gursel I, Sariyildiz S, Akin Ö, Stouffs R. Modeling and visualization of lifecycle building performance assessment. *Adv Eng Inform*. 2009;23(4):396–417. <https://doi.org/10.1016/j.aei.2009.06.010>.
19. Brusaporci S, Maiezza P, Tata A. A framework for architectural heritage HBIM semantization and development. *Int Arch Photogramm Remote Sens Spatial Inf Sci*. 2018;XLII-2:179–84. <https://doi.org/10.5194/isprs-archives-XLII-2-179-2018>.
20. Fiorini G, Friso I, Balletti C. A geomatic approach to the preservation and 3D communication of urban cultural heritage for the history of the city: the journey of Napoleon in Venice. *Remote Sens*. 2022;14:14. <https://doi.org/10.3390/rs14143242>.
21. Logothetis S, Delinasiou A, Stylianidis E. Building information modeling for cultural heritage: a review. *ISPRS Ann Photogramm Remote Sens Spatial Inf Sci*. 2015;II-5/W3:177–83. <https://doi.org/10.5194/isprs-annals-II-5-W3-177-2015>.
22. Chevrier C, Charbonneau N, Grussenmeyer P, Perrin JP. Parametric documenting of built heritage: 3D virtual reconstruction of architectural details. *Int J Archit Comput*. 2010;8(2):135–50. <https://doi.org/10.1260/1478-0771.8.2.135>.
23. Ramos Sánchez JA, Cruz Franco PA, de la Rueda Márquez Plata A. Achieving universal accessibility through remote virtualization and digitization of complex archaeological features: a graphic and constructive study of the Columbarios of Merida. *Remote Sens*. 2022;14:14. <https://doi.org/10.3390/rs14143319>.
24. Guarneri A, Guidi G, Tucci G, Vettore A. Towards automatic modeling for cultural heritage applications. *The International Archives of the Photogrammetry, Remote Sensing and Spatial Information Sciences*. 2003;XXXIV, Part 5/W12:176–81.
25. Carvajal DAL, Morita MM, Bilmes GM. Virtual museums. Captured reality and 3D modeling. *J Cult Herit*. 2020;45:234–9. <https://doi.org/10.1016/j.culher.2020.04.013>.
26. Remondino F, Girardi S, Rizzi A, Gonzo L. 3D modeling of complex and detailed cultural heritage using multi-resolution data. *Assoc Comput Mach*. 2009;2:1–20. <https://doi.org/10.1145/1551676.1551678>.
27. Elkhachy I. 3D Structure from 2D dimensional images using structure from motion algorithms. *Sustainability*. 2022;14:9. <https://doi.org/10.3390/su14095399>.
28. Elkhachy I. Modeling and visualization of three dimensional objects using low-cost terrestrial photogrammetry. *Int J Archit Herit*. 2020;14(10):1456–67. <https://doi.org/10.1080/15583058.2019.1613454>.
29. Fiz JI, Martín PM, Cuesta R, Subías E, Codina D, Cartes A. Examples and results of aerial photogrammetry in archeology with UAV: geometric documentation, high resolution multispectral analysis, models and 3D printing. *Drones*. 2022;6:3. <https://doi.org/10.3390/drones6030059>.
30. Remondino F, Guarneri A, Vettore A. 3D modeling of close-range objects: photogrammetry or laser scanning. *Proc SPIE*. 2004;5665:216–25. <https://doi.org/10.1117/12.586294>.
31. Yastikli N. Documentation of cultural heritage using digital photogrammetry and laser scanning. *J Cult Herit*. 2007;8(4):423–7. <https://doi.org/10.1016/j.culher.2007.06.003>.
32. Barsanti SG, Remondino F, Visintini D. Photogrammetry and laser scanning for archaeological site 3D modeling—Some critical issues. In: *CEUR Workshop Proceedings*. 2012;948:B1–10.
33. Adami A, Fregonese L, Lattanzi D, Mazzeri A, Rossignoli O, Scala B. A multi-disciplinary conservation project for the Cavallerizza Courtyard, Palazzo Ducale di Mantova. *Heritage*. 2019;2(2):1441–59. <https://doi.org/10.3390/heritage2020091>.
34. Guarneri A, Remondino F, Vettore A. Digital photogrammetry and TLS data fusion applied to Cultural Heritage 3D modeling. *Int Arch Photogramm Remote Sens Spatial Inf Sci*. 2012;36(5):1–6.
35. Hu Y, Feng B, Hou M. A study on the detection of bulging disease in ancient city walls based on fitted initial outer planes from 3D point cloud data. *Herit Sci*. 2023;11(1):10. <https://doi.org/10.1186/s40494-022-00856-6>.
36. Haznedar B, Bayraktar R, Ozturk AE, Arayici Y. Implementing PointNet for point cloud segmentation in the heritage context. *Herit Sci*. 2023;11(1):2. <https://doi.org/10.1186/s40494-022-00844-w>.
37. Guo M, Sun M, Pan D, Wang G, Zhou Y, Yan B, Fu Z. High-precision deformation analysis of yingxian wooden pagoda based on UAV image and terrestrial LiDAR point cloud. *Herit Sci*. 2023;11(1):1. <https://doi.org/10.1186/s40494-022-00833-z>.
38. Lerma-Cobo F, Romero-Manchado A, Enríquez C, Ramos MI. A high detail UAS-based 3D model of the Torre Benzalá in Jaén, Spain. *Herit Sci*. 2022;10(1):203. <https://doi.org/10.1186/s40494-022-00835-x>.
39. Martínez-Carricondo P, Carvajal-Ramírez F, Yero-Paneque L, Agüera-Vega F. Combination of HBIM and UAV photogrammetry for modelling and documentation of forgotten heritage. Case study: Isabel II dam in Nijar (Almería, Spain). *Herit Sci*. 2021;9(1):95. <https://doi.org/10.1186/s40494-021-00571-8>.
40. Mohammadi M, Rashidi M, Mousavi V, Karami A, Yu Y, Samali B. Quality evaluation of digital twins generated based on UAV photogrammetry and TLS: bridge case study. *Remote Sens*. 2021. <https://doi.org/10.3390/rs13173499>.
41. Moon D, Chung S, Kwon S, Seo J, Shin J. Comparison and utilization of point cloud generated from photogrammetry and laser scanning: 3D world model for smart heavy equipment planning. *Autom Constr*. 2019;98:322–31. <https://doi.org/10.1016/j.autcon.2018.07.020>.
42. Laux D, Henk A. Terrestrial laser scanning and fracture network characterization—Perspectives for a (semi-) automatic analysis of point cloud data from outcrops. *Z Dtsch Ges Geowiss*. 2015. <https://doi.org/10.1127/1860-1804/2015/0089>.
43. Riegl LMS. *RiSCAN Pro manual*. Horn, Austria; 2013.
44. Tysiac PS. Adalberd church 3D point model. Gdańsk Univ Technol. 2023. <https://doi.org/10.34808/6hsv-ds40>.
45. Charles A, Loucks L, Berkes F, Armitage D. Community science: a typology and its implications for governance of social-ecological systems. *Environ Sci Policy*. 2020;106:77–86. <https://doi.org/10.1016/j.envsci.2020.01.019>.

## Publisher's Note

Springer Nature remains neutral with regard to jurisdictional claims in published maps and institutional affiliations.

